

RSC Advances



This is an *Accepted Manuscript*, which has been through the Royal Society of Chemistry peer review process and has been accepted for publication.

Accepted Manuscripts are published online shortly after acceptance, before technical editing, formatting and proof reading. Using this free service, authors can make their results available to the community, in citable form, before we publish the edited article. This *Accepted Manuscript* will be replaced by the edited, formatted and paginated article as soon as this is available.

You can find more information about *Accepted Manuscripts* in the [Information for Authors](#).

Please note that technical editing may introduce minor changes to the text and/or graphics, which may alter content. The journal's standard [Terms & Conditions](#) and the [Ethical guidelines](#) still apply. In no event shall the Royal Society of Chemistry be held responsible for any errors or omissions in this *Accepted Manuscript* or any consequences arising from the use of any information it contains.

ARTICLE

Organic molecule controlled synthesis of three-dimensional rhododendra-like cobalt sulfide hierarchitectures as counter electrodes for dye-sensitized solar cells

Cite this: DOI: 10.1039/x0xx00000x

Received 00th January 2012,
Accepted 00th January 2012

DOI: 10.1039/x0xx00000x

www.rsc.org/

Lijuan Sun,^a Yu Bai,^{a*} Kening Sun^{a,b*}

Three-dimensional rhododendra-like cobalt sulfide (CoS) hierarchitectures have been prepared via a simple hydrothermal approach based on organic molecule directing method. The growth of CoS nanostructure is described in detail and the performance of the dye-sensitized solar cell based on the CoS counter electrode is evaluated. The hierarchitectures are constructed with two-dimensional nanosheets. The growth of nanosheet is induced by cysteine and ethylenediamine, and the thickness of the nanosheet is found to be dependent on the reaction time. Electrochemical measurements reveal that the rhododendra-like CoS is a superior catalyst towards the reduction of triiodide (I_3^-). When it is used as counter electrode for dye-sensitized solar cell, the power conversion efficiency is up to 3.53%, which is comparable to the efficiency of the cell with Pt counter electrode (3.93%).

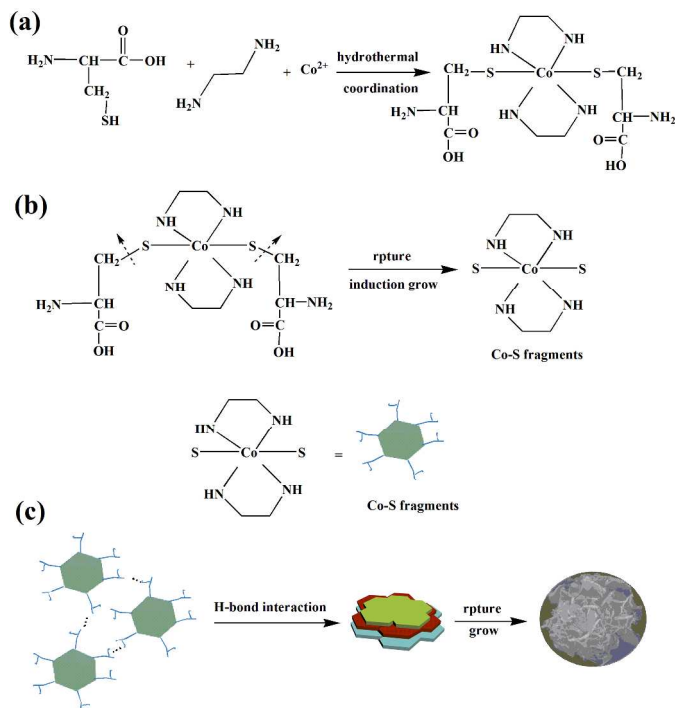
1. Introduction

Dye-sensitized solar cells (DSSCs) have attracted great attention during the last two decades owing to their simple fabrication processes, low cost of raw materials and relatively high power conversion efficiency (PCE).¹⁻³ A typical DSSC has a sandwich structure including a photoanode (metal oxide sensitized by dye molecules), a redox couple electrolyte (iodide/triiodide (I^-/I_3^-) is commonly used), and a counter electrode (CE). As an important component of DSSC, extensive research efforts have been devoted to the development of counter electrode.

Recently, nano-size CoS has been proposed as a new counter electrode material owing to its low-cost, simple preparation and excellent catalytic ability toward the reduction of triiodide (I_3^-) in DSSCs.⁴⁻⁹ Although materials with nano-size are favorable in terms of kinetics, their practical applications suffer from low thermodynamic stability which can lead to the fading of device efficiency.¹⁰ The optimization of the morphology and structure has been regarded as an effective way to overcome these drawbacks, thus improving catalytic ability without deteriorating mass-transfer kinetics. As a result, the 3D hierarchitectures assembled by nanostructures, in which the advantages of nano-size and micro-size can be combined, have been extensively explored.¹¹⁻¹⁴ More importantly, the hierarchical nanostructures can maintain a high

surface area, keep better permeability and stability, possess more active sites and low mass-transfer resistance, which are advantageous to the improvement of catalytic activity for electrode materials.¹⁵⁻¹⁹ However, developing a facile and template-free approach for the synthesis of high-purity hierarchical nanostructures with a well-defined morphology still remains a great challenge.

In this work, we design a simple, inexpensive, and environmentally benign approach to prepare the CoS with 3D rhododendra-like hierarchitectures. Considering the coordination ability of some organic molecules with special functional groups, l-cysteine ($HSCH_2CH(NH_2)COOH$) and ethylenediamine ($NH_2(CH_2)_2NH_2$) are chosen to control the morphology of the product. During the reaction process, l-cysteine not only acted as sulfur source but also induced the growth of nanosheet (Scheme 1). Simultaneously, the thickness of the nanosheet can be modified by varying the reaction time. When the as-prepared CoS was used as counter electrode, the PCE of DSSC was up to 3.53%, which is comparable to the efficiency of the DSSC with Pt electrode (3.93%). To the best of knowledge, there are few reports on the electrochemical study of CoS with well-defined 3D nanostructures in DSSCs. More importantly, this method can be used for the synthesis of other functional materials.



Scheme 1 Illustration of the proposed growth mechanism.

2. Experimental

2.1 Synthesis of CoS

The CoS hierarchitectures were synthesized by a facile one-pot hydrothermal route, with $\text{CoCl}_2 \cdot 6\text{H}_2\text{O}$, 1-cysteine and ethylenediamine as starting materials. In a typical experiment, 1 mmol $\text{CoCl}_2 \cdot 6\text{H}_2\text{O}$ (0.24 g) and 3 mmol 1-cysteine (0.36 g) were dissolved in 25 mL deionized water, then the mixture was stirred for 10 min, followed by the addition of 10 mL ethylenediamine. The resultant solution was transferred into a 100 mL Teflon-lined stainless steel autoclave. The autoclave was maintained at 160 °C for 6 h, and then cooled down to room temperature naturally. The resultant products were collected by centrifuge, and washed for five times with distilled water and anhydrous ethanol to remove possible residual reactant. The product was finally obtained after drying in a vacuum at 60 °C for 24 h.

2.2 Characterization and electrochemical measurements

The crystal structure was detected on a PANalytical diffractometer with $\text{Cu K}\alpha$ radiation at a scanning rate of 2°min^{-1} . The morphology and structure of the representative samples were examined by a field emission scanning electron microscope (FESEM, Hitachi S-8010) and transmission electron microscopy (TEM, FEI Tecnai G² F30). Electrochemical impedance spectroscopy (EIS) experiments for DSSCs were carried on electrochemical system (PARSTAT 2273, USA) in the dark under open circuit voltage condition. The measured frequency ranged from 0.05 Hz-100 kHz. The analyses of the impedance spectra were made with the ZSimpWin version 3.1.

The Tafel polarization measurements were carried out with symmetrical dummy cells, using electrochemical workstation (CHI660D, Chenhua, Shanghai). The current density-voltage performance (J - V) of the DSSCs were measured in one sun illumination (AM 1.5G, 100 mW cm^{-2}) with Newport (USA) solar simulator (300 W Xe source) and digital source meter (Keithley 2400, USA), at room temperature.

2.3 Device fabrication

To prepare CoS counter electrode, a mixture of CoS powders, P25 (Degussa, Germany), and a polyvinylidene fluoride (PVDF) binder with a 8:1:1 weight ratio in N-methyl pyrrolidone (NMP) were ground in mortar, and then the resultant homogenous CoS paste was coated onto a fluorine-doped tin oxide (FTO) glass substrate by doctor blading method. After drying at room temperature, electrodes were heated at 120 °C in vacuum for 12 h. The Pt counter electrode was prepared by heating 2 mg mL^{-1} solution of H_2PtCl_6 (Sigma) in isopropyl alcohol on FTO glass substrate at 400 °C for 30 min.

The photoanode was obtained through the sensitization of the 8 μm TiO_2 film with a 300 μM solution of Z907 (Solaronix SA, Switzerland) in acetonitrile/tert-butyl alcohol (1:1 volume ratio) for 16 h. Photoanode with active area of 0.2826 cm^2 and counter electrode were assembled in a sandwich configuration using a hot melting ring. The liquid electrolyte was composed of 0.03 M I_2 , 0.05 M LiI, 1 M 1, 2-dimethyl-3-propylimidazolium iodide (DMII), 0.1M guanidine isothiocyanate (GNCS) and 1 M 4-tert-butyl-pyridine (TBP) in acetonitrile. The electrolyte was injected into the aperture of counter electrode via vacuum back filling method. The photos of the device and electrode are given in the supporting information (Figure S1, Figure S2).

2. Results and discussion

According to the previous report,²⁰ it is quite difficult to obtain pure CoS because of the complex stoichiometric of cobalt chalcogenides. Encouragingly, as indicated in Fig. 1(a), the XRD pattern of the as-prepared CoS is of high purity, and all of the diffraction peaks can be assigned to CoS with a hexagonal structure (JCPDS no. 65-3418). The SEM image presented in Fig. 1(b) confirms the morphology of CoS is rhododendra-like. As shown in Fig. 1(c) and Fig. 1(d), a rhododendra-like structure is comprised of 2D nanosheets and the thickness of single nanosheet is about 10 nm. The rhododendra-like particles with typical diameter about 1 μm and the surface edges of these nanosheets are staggered just like ladder instead of aligned structure. In terms of kinetics, this framework is beneficial for the diffusion of electrolyte. Furthermore, the electrode-electrolyte contact area can be enlarged by the sheet-like structure. As displayed in Fig. 1(e), the low magnification TEM image further confirm the rhododendra-like structure is consisted of nanosheets. In addition, a careful examination of single petal by high resolution transmission electron microscopy (HRTEM, Fig. 1(f)) implies that the sheet-like structure is made up of many smaller crystallites with random orientation, suggesting that the primary polycrystalline nanosheets

was obtained due to the agglomeration of crystallites during the hydrothermal process.

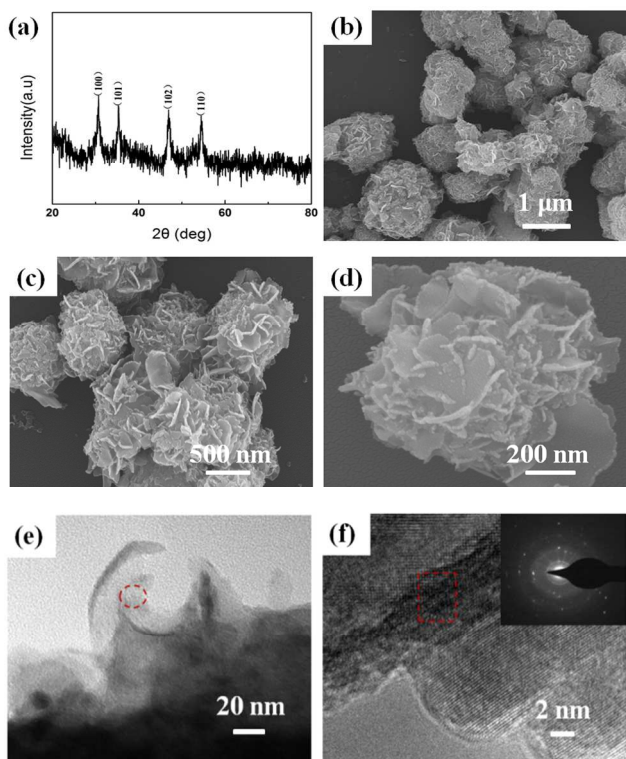


Fig. 1 (a) XRD patterns of the 3D rhododendra-like cobalt sulfide, (b, c, d) SEM images in different magnification, (e) TEM image of CoS, (f) HRTEM image and the corresponding SAED pattern (inset) of the individual nanosheet.

In order to understand the growth mechanism, further investigations have been conducted to track the time-dependent evolution of the morphology of the product. At the beginning of the reaction (reaction time: 4 h), a sphere-like product consisted of many fine irregular-shaped particles and smaller nanosheets (Fig. 2(a)) was formed. As shown in Fig. 2(b), after 8 h hydrothermal treatment, the nanosheets grew and enlarged gradually, but they were still wrapped by lots of nanoparticles. By further prolonging the reaction time to 10 h, a further growing for nanosheets can be observed, and many nanosheets stacked loosely, many macropores can be observed (Fig. 2(c)). It is worth notice that when the reaction time was increased to 12 h, the nanosheets became thicker and stacked into a dense sphere-like structure, as displayed in Fig. 2(d). This observation confirms that prolonging reaction time mainly increases the thickness of the nanosheet and facilitates the formation of dense sphere-like structure. Based on above results and discussion, we assume that the formation of CoS hierarchical structure comprises the following three main steps: (1) At the beginning of the reaction, the formation of the $\text{Co}(\text{en}, \text{cysteine})^{2+}$ complex due to the strong tendency of ethanediamine and cysteine molecule^{21,22} to coordinate Co^{2+} (Scheme 1(a)), (2) The growing of the polycrystalline nanosheet due to the inducing effect of functional groups from ligands (ethanediamine and cysteine) (Scheme 1(b)). (3) The further stacking of the nanosheets into a rhododendra-like structure induced

by the hydrogen bond interaction. Subsequently, the coordination bonds between the hydrosulfide group and Co^{2+} ruptured and CoS was assembled into the rhododendra-like structure²³ (Scheme 1(c)). It is well-known that the coordinating ability and polarity of solvent have greatly influences on the morphology of final product.²⁴ Particularly, due to the N-chelating behavior, amine molecule has played a significant role in the synthesis of transition metal compounds with different morphology, such as CdS, ZnSe, ZnTe.²⁵⁻²⁷ Therefore, during the synthesis process, the $\text{Co}(\text{en}, \text{cysteine})^{2+}$ complex may serve as a molecular template to control the growth of nanosheet as the previous literature reported.²³ In brief, herein, a reasonable mechanism is proposed for rhododendra-like CoS product, as declared in Scheme 1.

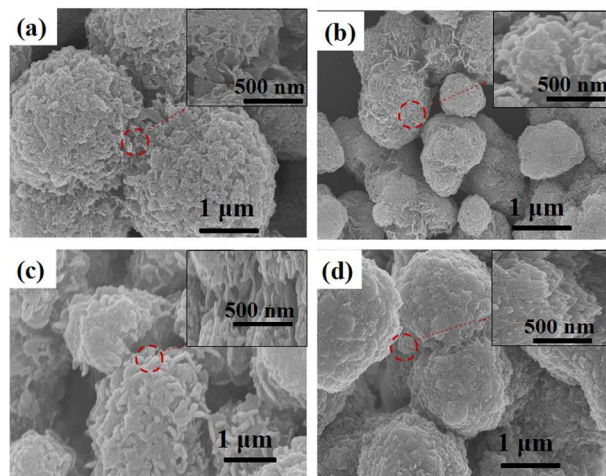


Fig. 2 SEM images of the CoS synthesized at 160°C for different time intervals: (a) 4 h, (b) 8 h, (c) 10 h, (d) 12 h.

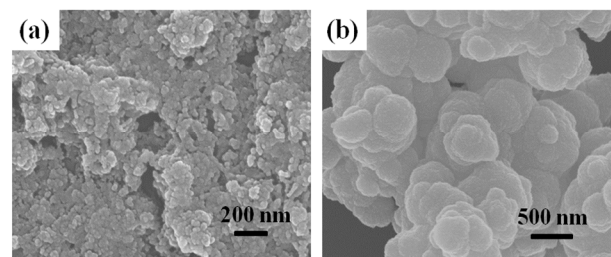


Fig. 3 SEM images of the CoS at different conditions: (a) L-cysteine = 0 mmol, Na_2S = 3 mmol, ethylenediamine = 10 mL. (b) L-cysteine = 3 mmol, ethylenediamine = 0 mL.

To further elaborate the effect of the two kinds of organic molecule on the crystal growth, several adjustments to the reaction conditions were made. As shown in Fig. 3(a), when the Na_2S and ethylenediamine were used as starting materials, particles with irregular shape were observed. This is ascribed to the fast release of S^{2-} leading to a fast nucleation and agglomeration. On the other hand, when L-cysteine was utilized as sulfur source without addition of ethylenediamine, sphere-like product with a size of about 500 nm was obtained (Fig. 3(b)). This is because the $-\text{SH}$ in L-cysteine molecule can coordinate to Co^{2+} (complexing effect), which effectively limits nucleation rate and can be in favor of the formation

of sphere-like CoS. The above results further demonstrate the coexistence of the ethylenediamine and in the reaction system are necessary for the formation of 3D rhododendra-like structure.

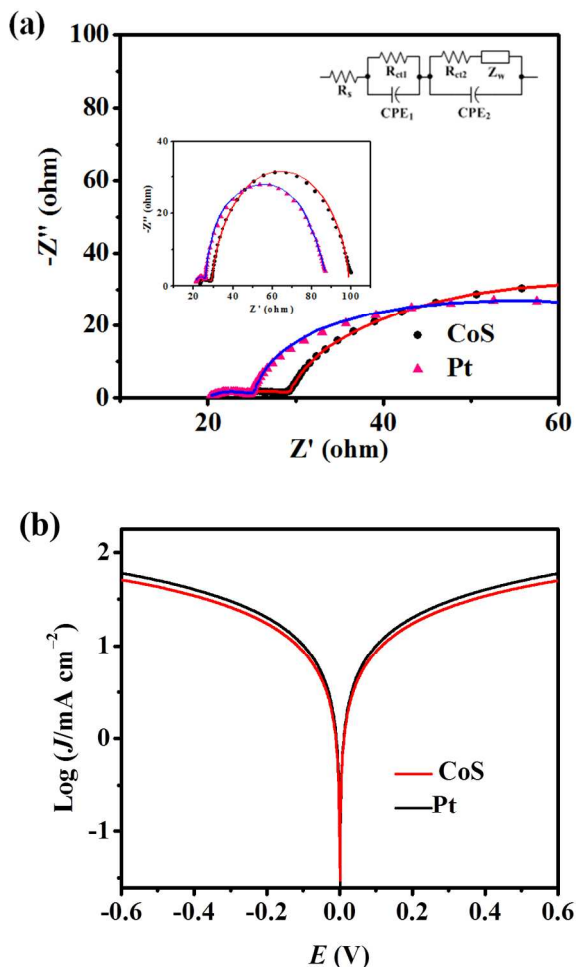


Fig. 4 (a) Nyquist plots of the DSSCs with CoS and Pt electrodes, respectively. The lines are corresponding to the simulated data of CoS and Pt electrodes, respectively. The inset shows the equivalent circuit model. (b) Tafel polarization curves of symmetrical cells with Pt and CoS electrodes.

In order to characterize the catalytic activity of different materials, EIS experiments were carried out on DSSCs with CoS and Pt counter electrodes. According to the previous reports,^{28,29} for each of the Nyquist plots, the semicircles (from high frequency to low frequency) represent the electrocatalytic resistance at the interface between the electrolyte and the CE (R_{ct1}) and the charge-transfer resistance at the interface of $\text{TiO}_2/\text{dye}/\text{electrolyte}$ (R_{ct2}). The detailed explanations have been given in supporting information (Figure S3). In order to compare the electrochemical performance of counter electrodes, the values of R_{ct1} are mainly investigated here. As shown in Fig. 4(a), the simulated R_{ct1} of CoS electrode is 6.54Ω , which is a little higher than that of the Pt electrode (5.43Ω). It indicates that the CoS electrode has a similar catalytic activity with Pt electrode for the reduction of I_3^- .³⁰ The result implies the potential application of

the three-dimensional rhododendra-like CoS as a low cost counter electrode material in DSSCs.

To further characterize the activity of different CEs, Tafel polarization measurements were carried out by using symmetrical dummy cells. As displayed in Fig. 4(b), the anodic and cathodic branches of the CoS electrode show a similar slope with the Pt electrode, indicating the presence of a similar exchange current density on the electrode surfaces. These results confirm that the CoS electrode is sufficient to catalyze the reduction of triiodide.³¹ This can be attributed to the more reaction active sites which arises from the special rhododendra-like structure.³² Furthermore, the electrochemical stability tests were carried out, demonstrating that the CoS electrode has a good electrochemical stability (Figure S4).

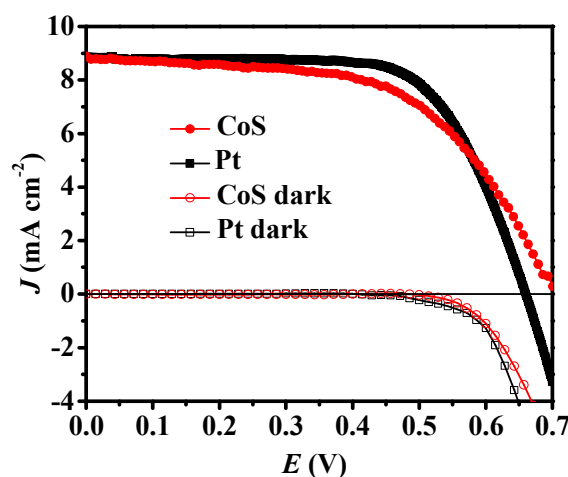


Fig. 5 Current density-voltage (J - V) characteristics of CoS and Pt based DSSCs under one sun illumination (AM 1.5G, 100 mW cm^{-2}) and in the dark.

Both current density-voltage curves for DSSCs with CoS and Pt CEs are given in Fig. 5, and the corresponding photovoltaic performance parameters are summarized in Table 1. As shown in Table 1, when the rhododendra-like CoS is used as the counter electrode, the photovoltaic parameters of the corresponding DSSC are as follows: $V_{oc} = 0.70 \text{ V}$, $J_{sc} = 8.87 \text{ mA cm}^{-2}$, $FF = 0.57$, $PCE = 3.53\%$. Clearly, the DSSC assembled CoS CE generates similar parameters to the DSSC with Pt CE ($V_{oc} = 0.66 \text{ V}$, $J_{sc} = 9.03 \text{ mA cm}^{-2}$, $FF = 0.66$, $PCE = 3.95\%$). It is noted that the fill factor of the DSSC with CoS CE is slightly lower than that of the Pt based cell, which may be caused by the low conductivity of CoS electrode.

Table 1 Photovoltaic parameters of the DSSCs based on CoS and Pt CEs

Counter electrode	V_{oc} (V)	J_{sc} (mA cm^{-2})	FF	PCE (%)
CoS	0.70	8.87	0.57	3.53
Pt	0.66	9.03	0.66	3.93

Conclusions

In conclusion, we present a CoS material with unique 3D rhododendra-like hierarchitectures as a high efficient counter electrode for dye-sensitized solar cells. It is synthesized via a simple hydrothermal approach based on organic molecule directing method. This strategy not only avoids the emergence of noxious H₂S, but also controls the growth of 3D rhododendra-like hierarchitectures, effectively. When the as-prepared CoS was used as the counter electrode for DSSC, the PCE is up to 3.53%, which is comparable to the efficiency of the device with Pt electrode (3.93%). This excellent electrochemical performance is related with the special 3D rhododendra-like architectures of CoS counter electrode. More importantly, this 3D rhododendra-like CoS hierarchitectures exhibit a very promising performance for catalysis and energy storage application.

Acknowledgements

This project is supported by the National Natural Science Foundation of China (No. 51203036), the China Postdoctoral Science Special Foundation (2013T60380), the China Postdoctoral Science Foundation (2012M520748), and the “Young Talent Program” of Harbin Institute of Technology.

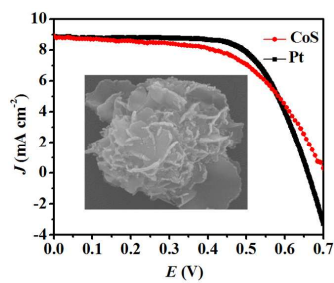
Notes and references

^aAcademy of Fundamental and Interdisciplinary Sciences, Harbin Institute of Technology, Harbin, 150001, China Fax: +86 451 86412153; Tel: +86 451 86412153; E-mail: keningsunhit@126.com; yu.bai@hit.edu.cn.

^bState Key Laboratory of Urban Water Resource and Environment, Harbin Institute of Technology, Harbin, 150090, China.

- 1 B. O'regan, M. Grätzel, *Nature*, 1991, **353**, 737–740.
- 2 A. Hagfeldt, G. Boschloo, L. Sun, L. Kloo, H. Pettersson, *Chem. Rev.*, 2010, **110**, 6595–6663.
- 3 A. Yella, H. W. Lee, H. N. Tsao, C. Yi, A. K. Chandiran, M. K. Nazeeruddin, E. W. G. Diau, C. Y. Yeh, S. M. Zakeeruddin, M. Grätzel, *Science*, 2011, **334**, 629–634.
- 4 M. K. Wang, A. M. Anghel, B. Marsan, M. Grätzel, *J. Am. Chem. Soc.*, 2009, **131**, 15976–15977.
- 5 C. W. Kung, H. W. Chen, C. Yu. Lin, *ACS Nano*, 2012, **6**, 7016–7025.
- 6 J. Y. Lin, J. H. Liao, S. W. Chou, *Electrochimica Acta*, 2011, **56**, 8818–8826.
- 7 L. L. Zhang, H. K. Mulmudi, S. K. Batabyal, Y. M. Lam, S. G. Mhaisalkar, *Phys. Chem. Chem. Phys.*, 2012, **14**, 9906–9911.
- 8 S. H. Chang, M. D. Lu, Y. L. Tung, H. Y. Tuan, *ACS Nano*, 2013, **7**, 9443–9451.
- 9 J. Y. Lin, S. Y. Tai, S. W. Chou, *J. Phys. Chem. C.*, 2014, **118**, 823–830.
- 10 Y. C. Z. Zhong, D. Wang, W. U. Wang, C. M. Lieber, *Nano Lett.*, 2003, **3**, 149–152.
- 11 R. C. Jin, J. S. Liu, Y. B. Xu, G. H. Li, G. Chen, *J. Mater. Chem. A*, 2013, **1**, 7995–7999.
- 12 Z. Q. Liu, L. X. Ding, Z. L. Wang, Y. C. Mao, S. L. Xie, Y. M. Zhang, G. R. Li, Y. X. Tong, *CrystEngComm.*, 2012, **14**, 2289–2295.

- 13 X. Y. Zhang, Y. H. Zheng, D. G. McCulloch, L. Y. Yeo, J. R. Friend, D. R. MacFarlane, *J. Mater. Chem. A*, 2014, **2**, 2275–2282.
- 14 A. Kargar, K. Sun, Y. Jing, C. Choi, H. Jeong, G. Y. Jung, S. Jin, D. L. Wang, *ACS Nano*, 2013, **7**, 9407–9415.
- 15 Y. C. Z. Zhong, D. Wang, W. U. Wang, C. M. Lieber, *Nano Lett.*, 2003, **3**, 149–152.
- 16 M. T. Niu, F. Huang, L. F. Cui, P. Huang, Y. L. Yu, Wang, S. Y., *ACS Nano*, 2010, **4**, 681–688.
- 17 W. J. Liang, B. D. Yuhas, P. D. Yang, *Nano Lett.*, 2009, **9**, 892–896.
- 18 B. G. Choi, S. J. Chang, Y. B. Lee, J. S. Bae, H. J. Kim, Y. S. Huh, *Nanoscale*, 2012, **4**, 5924–5930.
- 19 J. P. Bosco, K. Sasaki, M. Sadakane, W. Ueda and J. G. Chen, *Chem. Mater.*, 2010, **22**, 966–967.
- 20 Z. Yang, C. Y. Chen, H. T. Chang, *J. Power Sources*, 2011, **196**, 7874–7877.
- 21 S. J. Bao, C. M. Li, C. X. Guo, Y. Qiao, *J. Power Sources*, 2008, **180**, 676–681.
- 22 S. H. Yu, M. Yoshimura, *Adv. Mater.*, 2002, **14**, 296–300.
- 23 B. Zhang, X. C. Ye, We. Y. Hou, Y. Zhao, Y. Xie, *J. Phys. Chem. B*, 2006, **110**, 8978–8985.
- 24 C. H. Lai, K. W. Huang, J. H. Cheng, C. Y. Lee, B. J. H, L. J. C, *J. Mater. Chem.*, 2010, **20**, 6638–6645.
- 25 Y. D. Li, H. W. Liao, Y. Ding, Y. T. Qian, L. Yang, G. E. Zhou, *Chem. Mater.*, 1998, **10**, 2301–2303.
- 26 W. T. Yao, S. H. Yu, X. Y. Huang, J. Jiang, L. Q. Zhao, L. Pan, J. Li, *Adv. Mater.*, 2005, **17**, 2799–2802.
- 27 X. Y. Huang, J. Li, Y. Zhang, A. Mascarenhas, *J. Am. Chem. Soc.*, 2003, **125**, 7049–7055.
- 28 Q. Wang, J-E. Moser, and M. Grätzel, *J. Phys. Chem. B*, 2005, **109**, 14945–14953.
- 29 F. Shao, J. Sun, L. Gao, J. Z. Chen, S. W. Yang, *RSC Adv.*, 2014, **4**, 7805–7810.
- 30 F. Fabregat-Santiago, J. Bisquert, E. Palomares, L. Otero, D. B. Kuang, S. M. Zakeeruddin, M. Grätzel, *J. Phys. Chem. C*, 2007, **111**, 6550–6560.
- 31 M. X. Wu, X. Lin, A. Hagfeldt, T. L. Ma, *Angew. Chem. Int. Ed.*, 2011, **50**, 3520–3524.
- 32 Q. H. Wang, L. F. Jiao, Y. Han, H. M. Du, W. X. Peng, Q. N. Huan, D. W. Song, Y. C. Si, Y. J. Wang, H. T. Yuan, *J. Phys. Chem. C*, 2011, **115**, 8300–8304.



Organic molecule controlled synthesis of three-dimensional rhododendra-like CoS and its application as counter electrode in DSSCs.